

# Current Biology

## A corollary discharge mediates saccade-related inhibition of single units in mnemonic structures of the human brain

### Highlights

- Single-unit activity in the human hippocampus is modulated with saccades
- This single-unit activity modulation is dominated by inhibition
- The magnitude of modulation is correlated with peri-saccadic-evoked response amplitude
- Human mesial temporal lobe structures receive a corollary discharge during saccades

### Authors

Chaim N. Katz, Andrea G.P. Schjetnan, Kramay Patel, ..., Suneil K. Kalia, Katherine D. Duncan, Taufik A. Valiante

### Correspondence

taufik.valiante@uhn.ca

### In brief

Katz et al. characterize single-unit activity during saccadic eye movements in the human mesial temporal lobe. They demonstrate that this activity contains directional information and is inhibitory. These findings lead them to conclude that human memory structures receive a corollary discharge mediated by a circuit including the nucleus reuniens.



Article

# A corollary discharge mediates saccade-related inhibition of single units in mnemonic structures of the human brain

Chaim N. Katz,<sup>1,2,9,11,13</sup> Andrea G.P. Schjjetnan,<sup>1,9,13</sup> Kramay Patel,<sup>1,2,3,9,13</sup> Victoria Barkley,<sup>1,9</sup> Kari L. Hoffman,<sup>4</sup> Suneil K. Kalia,<sup>1,5,9,10</sup> Katherine D. Duncan,<sup>7</sup> and Taufik A. Valiante<sup>1,2,5,6,8,9,10,12,14,15,\*</sup>

<sup>1</sup>Krembil Brain Institute, Toronto Western Hospital (TWH), Toronto, ON M5T 1M8, Canada

<sup>2</sup>Institute of Biomedical Engineering, University of Toronto, Toronto, ON M5S 3G9, Canada

<sup>3</sup>Faculty of Medicine, University of Toronto, Toronto, ON M5S 1A8, Canada

<sup>4</sup>Department of Psychology, Vanderbilt University, Nashville, TN 37240, USA

<sup>5</sup>Division of Neurosurgery, Department of Surgery, University of Toronto, Toronto, ON M5S 1A1, Canada

<sup>6</sup>Institute of Medical Sciences, University of Toronto, Toronto, ON M5S 1A8, Canada

<sup>7</sup>Department of Psychology, University of Toronto, Toronto, ON M5S 3G3, Canada

<sup>8</sup>Electrical and Computer Engineering, University of Toronto, Toronto, ON M5S 3G4, Canada

<sup>9</sup>CRANIA, University Health Network and University of Toronto, Toronto, ON M5G 2A2, Canada

<sup>10</sup>The KITE Research Institute, University Health Network, Toronto, ON M5G 2A2, Canada

<sup>11</sup>Faculty of Medicine, University of Calgary, Calgary, AB T2N 4N1, Canada

<sup>12</sup>Max Planck-University of Toronto Center for Neural Science and Technology, Toronto, ON, Canada

<sup>13</sup>These authors contributed equally

<sup>14</sup>Twitter: @neuron2brain

<sup>15</sup>Lead contact

\*Correspondence: [taufik.valiante@uhn.ca](mailto:taufik.valiante@uhn.ca)  
<https://doi.org/10.1016/j.cub.2022.06.015>

## SUMMARY

Despite the critical link between visual exploration and memory, little is known about how neuronal activity in the human mesial temporal lobe (MTL) is modulated by saccades. Here, we characterize saccade-associated neuronal modulations, unit-by-unit, and contrast them to image onset and to occipital lobe neurons. We reveal evidence for a corollary discharge (CD)-like modulatory signal that accompanies saccades, inhibiting/exciting a unique population of broad-/narrow-spiking units, respectively, before and during saccades and with directional selectivity. These findings comport well with the timing, directional nature, and inhibitory circuit implementation of a CD. Additionally, by linking neuronal activity to event-related potentials (ERPs), which are directionally modulated following saccades, we recontextualize the ERP associated with saccades as a proxy for both the strength of inhibition and saccade direction, providing a mechanistic underpinning for the more commonly recorded saccade-related ERP in the human brain.

## INTRODUCTION

Humans rely on vision to understand their environment,<sup>1,2</sup> and their primary tool for exploration is the saccade<sup>3,4</sup>—a ballistic movement of the eyes from one fixation point to another. Given the importance of saccades, it may seem intuitive that they are inextricably linked to memory<sup>5–12</sup> and are associated with prominent electrophysiological responses<sup>13–15</sup> in memory-related, mesial temporal lobe (MTL) structures. Anatomical connections between MTL and oculomotor systems have been investigated.<sup>12</sup> However, the cellular mechanisms through which oculomotor structures influence the human MTL remain largely unknown, hindering the understanding of *how* eye movements interact with the memory system. In vision, saccade-related motor signals, in the form of a corollary discharge (CD), prepare the brain for the sensory consequences of a planned movement.<sup>16,17</sup> Our and others' recent intracranial electroencephalographic (iEEG) recordings provide preliminary clues that saccade-related

responses in the human MTL may also reflect a CD-like signal. Specifically, we previously demonstrated that saccade-related MTL event-related potentials (ERPs) are unlikely to reflect visual exafference; visual and saccade-related activity displayed different oscillatory profiles, and saccade-related modulation was time locked to the onset of the motor (saccade) initiation and not the onset of new visual information (fixation).<sup>15</sup> Moreover, saccadic modulation of MTL electrophysiology has been shown to persist in the dark,<sup>18–20</sup> again suggesting that the MTL modulation likely arises from internally generated signals, like a CD.

In the most rudimentary implementation of a CD, a copy of the initiating motor command suppresses the sensation produced by the intended motor action.<sup>21–23</sup> In this implementation, the circuit motif consists of axon collaterals of primary motor neurons synapsing onto inhibitory interneurons, which inhibit sensory neurons during the movement.<sup>16,17</sup> Increasingly complex variations on this motif have been presented for the CD-like



discharges across the phylogenetic tree; however, inhibition remains a key mechanism by which CDs mediate their effects.<sup>17</sup> Indeed, within the taxonomy for CDs proposed by Crapse and Sommer, the saccadic inhibition/suppression of visual cortical excitability<sup>24</sup> comports well with the inhibition and sensory filtering function of a lower-order CD.

This saccadic suppression is considered a requirement for registering a stable visual percept of the world by blocking noisy visual input during ballistic eye movements (although alternative hypotheses exist for the observed saccadic suppression<sup>25</sup>). Of note, one group modified target placements during saccades to tease apart saccadic suppression's role in vision, where targets were displaced during a saccade. Human subjects could only detect the move if the target is blanked (i.e., briefly removed from the screen) prior to or during the saccade.<sup>26</sup> Additionally, blinking during a saccade to the displaced target, subjects were less likely to perceive target differences than when it is exogenously blanked.<sup>27</sup> Deubel et al. concluded that internally generated saccades contain an assumption of visual stability. When the external blanking condition is introduced, an extra-retinal signal is recalled to maintain a spatial, temporal relationship between targets before and after a saccade. Studies such as this support the functional importance of CD-mediated saccade suppression, in that information retained about the visual world during a saccade depend on internally and externally generated signals.

CDs may also play a role in amplifying visual responses during the subsequent fixation, where in the visual cortex enhanced neuronal activity follows a saccade.<sup>28,29</sup> This amplification of sensory responses is not isolated to eye movements. For example, when a rodent voluntarily initiates a motor act before visual sensory information is available, behavioral performance was also enhanced.<sup>30</sup> The findings support the concept that this copy of the motor command or CD can amplify behavioral responses.<sup>3</sup>

Additionally, CDs are thought to help produce a stable visual percept by dynamically shifting receptive fields in anticipation of ensuing eye movements (for a full review, see Wurtz<sup>31</sup>), suggesting they contain information about the direction and magnitude of ensuing saccades. Such a higher-order CD facilitates the transformation of the motor signal to visual coordinates necessary for anticipatory adjustments of neuronal receptive fields and updating spatial locations.<sup>21</sup> Such a function is well exemplified by its disruption; inhibiting the mediodorsal nucleus, a known node in a higher-order CD circuit, degraded non-human primate's (NHP) conscious perception of a target shift.<sup>32</sup>

From a pathological perspective, alteration of visual CDs have been proposed to accompany various neuropsychiatric conditions. Specifically, visual errors appear to correlate with the severity of the disease. Both delusional states in otherwise healthy individuals and psychosis in those with schizophrenia are accompanied by disrupted performance in tasks thought to involve visual<sup>33–35</sup> and auditory<sup>36</sup> CDs. In Parkinson's disease, disease severity correlated with increased errors during a saccade task.<sup>37</sup> Finally, various studies have even shown that eye movements may be predictive of different stages of neurological diseases.<sup>38,39</sup> For example, individuals with early stage Alzheimer's disease displayed an impaired compensation for distorted optic flow while making eye movements.<sup>40</sup>

Given the functional significance of CDs and only circumstantial iEEG evidence that a CD mediates saccade-related MTL

modulations in humans,<sup>14,15,41</sup> we seek to provide cellular level support for this hypothesis.<sup>42</sup> For this, we propose a framework based on the CD literature<sup>17,24,32,42,43</sup> to amass evidence of a CD in the human MTL. First, since CDs reflect the anticipatory modulation of sensory and/or higher-order structures, a saccade-related CD in the MTL must modulate firing rates before or during the saccade. Second, since most rudimentary CD circuits involve a prominent inhibition of sensory input, CD-related modulation of MTL activity should be largely inhibitory, evidenced by a decreased firing rate of putative pyramidal neurons and/or increased firing rate of putative inhibitory neurons. Third, there is extensive evidence of the modulation of single-unit activity (neuronal activity) in the MTL to visual stimuli.<sup>44–48</sup> Thus, any CD-related modulation of activity in the MTL should be distinct from the modulation associated with visual input. Finally, as part of an oculomotor circuit, CDs should represent the directional parameters of the ensuing movement. Thus, the CD-related modulation of neuronal activity within the MTL must demonstrate directional tuning (i.e., dissociable neuronal responses to ipsiversive and contraversive saccades).

We leverage the unique opportunity of recording neuronal activity from epilepsy patients undergoing diagnostic stereo-electroencephalography (sEEG) to characterize single-unit firing-rate changes that accompany saccades. While the participants visually searched natural scene images, we simultaneously recorded neuronal activity from the hippocampus and related MTL structures, along with eye movements. We utilized these recordings to characterize peri-saccadic neuronal activity according to our four criteria, both within the MTL and serendipitously obtained recordings from a control region, the occipital lobes, in two patients. Based on the above criteria and recognizing the limitations of human-related research, we provide correlative evidence for a saccade-related CD that modulates neuronal activity in the human hippocampus and other related MTL structures. From this, we propose a novel circuit that may underlie the cell-type-specific saccade-related responses we observe.

## RESULTS

### Search behavior

We used a task that involved visual search and recognition memory to elicit saccadic behavior. In this task, there was an encoding and retrieval session. Neural activity was analyzed during encoding sessions. Each encoding session consisted of 40 trials, starting with a fixation cross (1 s), followed by presenting a scene image. Four copies of one of two unrelated objects, i.e., targets, were embedded in the scene. Participants were instructed to view the individual, serially presented scene and find as many targets within the scene as possible (Figure 1A). During the encoding sessions, the median saccade duration was 31 ms. The saccade's horizontal direction was determined by subtracting its ending point from the starting point to determine if it was a leftward or rightward saccade. Saccades direction totals across subjects were not significantly different (paired t test,  $p = 0.63$ ) (Figure 1B).

### Neuronal activity within the MTL is modulated in the peri-saccadic interval

We recorded 524 neurons from MTL regions (hippocampus, amygdala, and parahippocampal cortex) across 11 patients

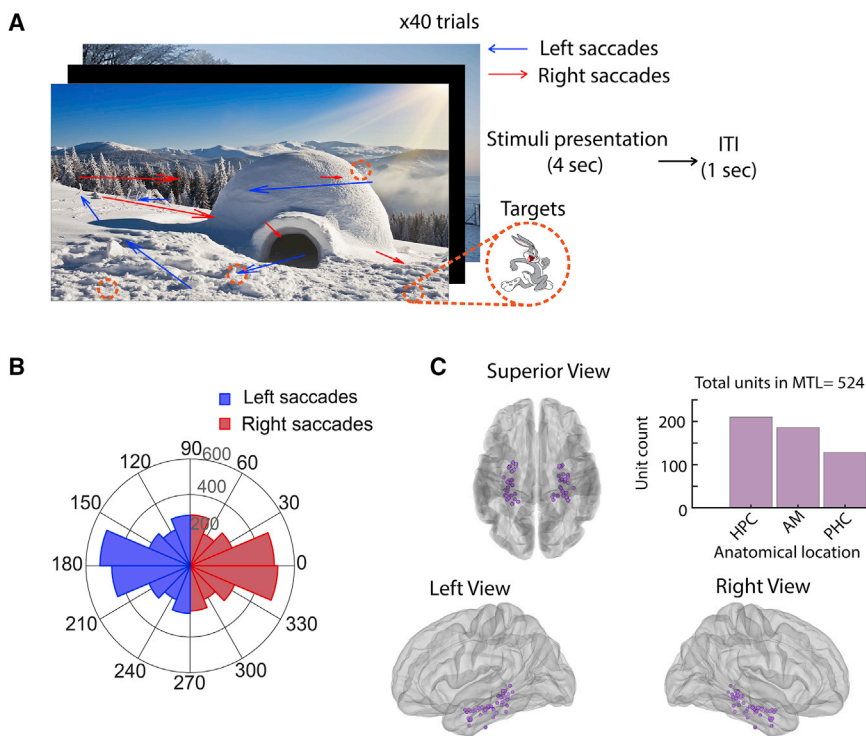


**Figure 1. Behavioral task and recording locations**

(A) Visual search task: participants searched for one of two target images (i.e., Bugs Bunny or Wile E. Coyote) in a series of pictures with natural scenes separated by a 1-s inter-trial interval (ITI). Example of saccade trajectories (arrows) with saccades classified as leftward (blue) or rightward (red) during 4 s of image presentation.

(B) Leftward and rightward saccade distributions. (C) Location of microwire bundles in different MTL areas. Insert: unit counts: HPC, hippocampus,  $n = 210$ ; AM, amygdala,  $n = 186$ ; PHC, parahippocampal cortex,  $n = 128$ .

(Figure 1C). Table 1 shows the distribution of neurons analyzed from the different areas. The density of waveforms of some example neurons is shown in Figure 2B. To determine whether saccades modulated single-unit activity in the MTL on a unit-by-unit basis, we analyzed the firing-rate changes in a 400 ms window surrounding each saccade and compared this activity with a matching null distribution generated by selecting random windows throughout the recording session (see Figure 2B and STAR Methods for details). We categorized single-unit activity as either increased, decreased, or no modulation in the firing rate. In doing so, we found that 6.7% (35/524 neurons) of MTL neurons were strongly modulated by the saccade (Figure S1A), with the majority demonstrating decreases in firing rates (31/35; Figure S1B).

In two participants, we had the unique opportunity to simultaneously record activity from the occipital lobe (Table 1; Figure S2). Overall, the various MTL structures presented similar results and therefore were grouped (Figure S3). Interestingly, a more significant (Fisher's exact test,  $p = 3.72E-24$ ) proportion of occipital lobe neurons were modulated around the time of saccades (46.4%, 58/125 neurons; Figure S2B). Since we have previously shown that ERPs related to saccades and image onset differ, we investigate MTL neurons response between these two conditions.<sup>15</sup>

### The units and the response timing of the saccades-related neuronal activity are distinct from those from image onset

The distinct nature of the ERPs associated with saccades and image onsets<sup>15</sup> suggests that the neuronal activity associated with saccades and image onset are likely to be separable. Specifically, ERPs associated with image onset were of an evoked

nature, suggesting that we should observe increases in neuronal activity related to image onset compared to inhibition-dominated changes in neuronal activity associated with saccades. Furthermore, the image-onset-evoked ERP's temporal evolution was slower, and thus, we would expect firing-rate changes to occur later.

To explore the potential differences between saccades and image onset, we analyzed peri-image onset responses in

a window of time between 200 and 1,700 ms after image onset.<sup>49</sup>

Neurons were classified as being modulated by image onset if their firing rate in this window significantly increased or decreased compared with the corresponding null distribution (Figure 2C). We found that 13.7% of the recorded MTL units were modulated by image onset ( $n = 72/524$ ; 67/524 increase; 5/524 decrease) (Figure 2D) and primarily demonstrated firing rate increases. Conversely, the majority of units that were modulated by saccades demonstrated decreases in their firing rate (31/35; Figure S1B).

We additionally found the population of neurons modulated by image onset to be distinct from those modulated around the time of saccades (Figure 2E). Furthermore, image-onset-modulated neurons demonstrated a peak increase in firing rates at  $650 \pm 100$  ms after image onset, well after the saccade-related units (Figure S1G). Thus, within the MTL, the units receiving visual information following image onset appear distinct from those responding to saccade-related information.

In the occipital cortex, a higher percentage of units than in the MTL were modulated following image onset (17.6%,  $n = 22/125$  in OC; 13.7%,  $n = 72/524$  in MTL) (Figure S2H). This difference was not significant ( $p = 0.26$ ). However, a larger proportion of occipital than MTL units were significantly modulated both following image presentation and during saccades (4%,  $n = 5/125$  in OC; 0%, 0/524 in MTL;  $p = 2.48E-04$ ).

Taken together, these results demonstrate a dichotomy between saccade-related and image-onset unit activity in the MTL, where the former is dominated by inhibition (see saccade-related modulation varies with direction and is predominantly inhibitory), begins and ends earlier, and is mediated by a signal that modulates a unique set of neurons. The latter feature of the saccade-related units in the MTL suggests that the

**Table 1. Patient summary table**

ID	Sex	Age	Sessions	No. saccades	HPC units	AM units	PHC units	OCC units	Total units
P89	F	45	1	538	13	14	30	0	57
P90	M	20	1	414	11	22	0	98	131
P91	F	59	1	463	2	3	0	0	5
P100	F	19	1	527	25	1	0	0	26
P101	F	25	1	625	32	6	10	0	48
P103	M	49	1	558	3	0	0	0	3
P107	F	64	1	641	0	9	1	0	10
P109	M	28	1	593	36	8	0	0	44
P116	M	28	1	555	21	58	0	0	79
P125	M	24	2	628	14	43	63	21	141
				821	8	22	22	6	58
P126	M	25	1	589	45	0	2	0	47
Total	–	–	–	–	210	186	128	125	649

Data for each participant are shown in the respective rows. HPC, hippocampus; AM, amygdala; PHC, parahippocampal cortex; OCC, occipital areas. See also [Figures S2](#) and [S3](#).

modulating signals associated with saccades within the MTL target distinct cell populations than units receiving visual input ([Figure 2E](#); see potential CD circuit for discussion of this).

### Saccadic modulation around saccade onset

In addition to the lack of overlap between image and saccade-related neurons, our previous finding that saccade-related ERPs are aligned to saccade onset rather than offset,<sup>15</sup> as well as the contemporary understanding of the arrival time of CDs relative to saccade onset,<sup>42</sup> together suggest neuronal activity should be modulated before and/or during a saccade.<sup>42</sup> To investigate this, we separated the modulated units in the MTL by their modulation type (increase or decrease). We obtained the maximum average firing-rate latency in a 400 ms window surrounding saccade onset for upmodulated units. Similarly, we found the latency of the minimum of the average firing rate in the same window for the downmodulated units. In doing so, we found that the trough of the firing-rate decrease occurred at  $-11 \pm 3$  ms relative to saccade onset, whereas the peak of the firing-rate increase occurred at  $0.5 \pm 12.57$  ms relative to saccade onset ([Figure S1C](#), inset; [Table S1](#)). Only downmodulated neurons were significantly different from zero (upmodulated, *t* test,  $p = 0.97$ ; downmodulated, sign rank,  $p = 0.001$ ), although these latency distributions were not different from each other (rank-sum,  $p = 0.33$ ). In summary, that the peri-saccadic modulation occurs before or during saccade initiation, well before the hippocampus would be expected to respond to changes in visual input, is consistent with a CD-like modulation of MTL units.<sup>45</sup>

Similarly, firing-rate troughs and peaks in the occipital lobe occurred at  $-11 \pm 3.2$  ms and  $0.33 \pm 15.7$  ms, respectively, relative to saccade onset. However, the rebound increase occurred at a longer latency ( $27 \pm 3$  ms; [Figure S2E](#)). Thus, saccade-associated neuronal activity modulation in both the MTL and occipital regions occur much earlier than image-onset modulations (see below and also Mormann et al.<sup>45</sup>). This pattern is consistent with the notion that this modulation of neuronal activity reflects the influence of a CD-like signal.<sup>50</sup>

### Saccade-related modulation varies with direction and is predominantly inhibitory

To determine how MTL neuronal activity is modulated in the peri-saccade interval, we explored how changes in firing rate are impacted by direction. We divided each unit into one of three categories: unmodulated, firing-rate increase, or firing-rate decrease. Of the saccade-modulated units in the MTL, we found that most units demonstrated a reduction in firing rate within the peri-saccadic window (88.6%,  $n = 31/35$ ), with the small remainder demonstrating increased firing rate (11.4%;  $n = 4$ ; [Figure S1B](#)).

In other saccade-related CD circuits, a CD signal conveys information regarding the ensuing saccade's direction and magnitude, likely facilitating anticipatory remapping of receptive fields in visual areas.<sup>51,52</sup> Thus, we would expect that if a CD signal mediates the MTL firing-rate modulation, we should observe directionally selective modulation in the peri-saccade interval. When separating by direction, a significantly ( $p = 5.4E-36$ ) larger fraction of modulated neurons were identified (20.4%,  $n = 107/524$ ) ([Figure 3B](#)), in addition to the 6.7% ( $n = 35/524$ ) of neurons that were classified as modulated when collapsing across saccade direction ([Figure S1A](#)), in line with previous work with primates (~20%).<sup>53</sup>

To further characterize this directional modulation, we classified these effects as (1) lateralized decreases (a decrease in firing rate for ipsiversive or contraversive saccades and no change for the opposite direction), (2) lateralized increases (an increase in firing rate for ipsiversive or contraversive saccades and no change for the opposite direction), and (3) mixed (increased firing rate in one direction, and decreased firing rate in the opposite direction). In the MTL, almost 70% of units showed lateralized decreases ( $n = 73/107$ ), consistent with one of our main findings, that units are largely inhibited in the peri-saccadic interval. A smaller subset of units had mixed modulation ([Figure 3C](#);  $n = 23/107$ ). Only a small population of neurons presented lateralized increases ( $n = 11/107$ ) ([Figure 3C](#)). In regard to the timing of these firing-rate changes, although lateralized decreases

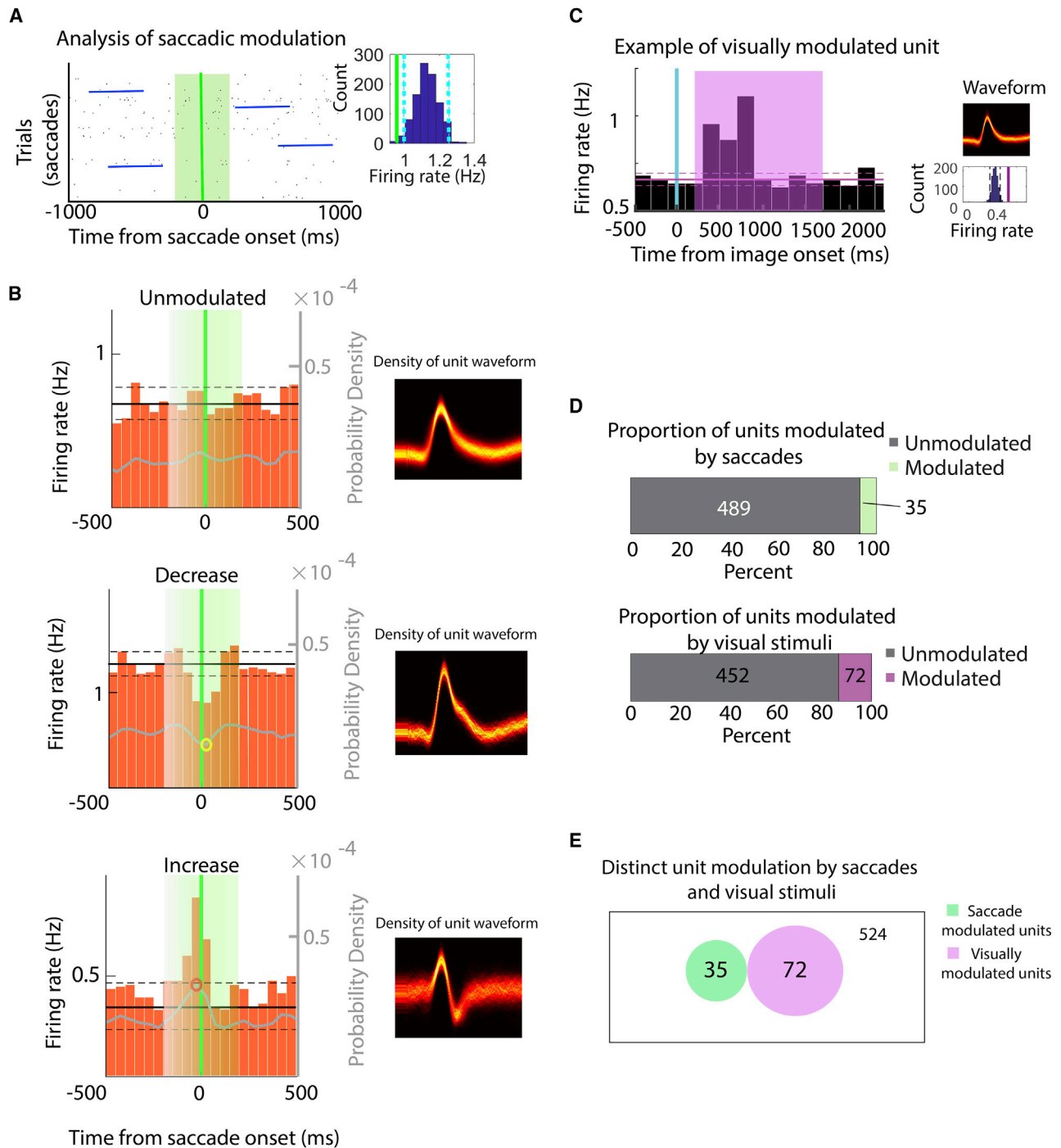


**Figure 2. Categories and distribution of modulated units for saccade and image onset**

(A) The relationship between saccades and neuronal activity was investigated by comparing spike counts during the 400 ms (mean of 8 bins of 50 ms each) peri-saccadic interval (green box) centered on saccade onset (green line) to those in control periods—bootstrapped aleatory 400 ms epochs from each specific unit (dark blue lines). Inset: null distribution of an example unit (dark blue). The green line represents the mean firing rate during the saccade period of the example neuron, and the cyan-dotted lines represent 95% confidence intervals from the random time windows. The mean firing rate (green line) is left of the lower confidence limit (cyan line), demonstrating a significant average decrease in firing rate during the peri-saccadic interval. Therefore, the unit is classified as “modulated.”

(B) Example of the different types of modulation observed. Modulated units were subdivided into those that (1) decreased their firing rate and (2) increased their firing rate during the peri-saccadic period (mean of 8 bins of 50 ms each). Firing-rate histograms of example units and mean waveform of each unit. Yellow circle, decrease trough; red, increase peak. Gray superimposed line indicates probability density (right y axis). Only units with statistically significant firings during the peri-saccadic periods (green box) were deemed to be modulated. Insets on the right show example spike waveforms represented as density plots.

(legend continued on next page)

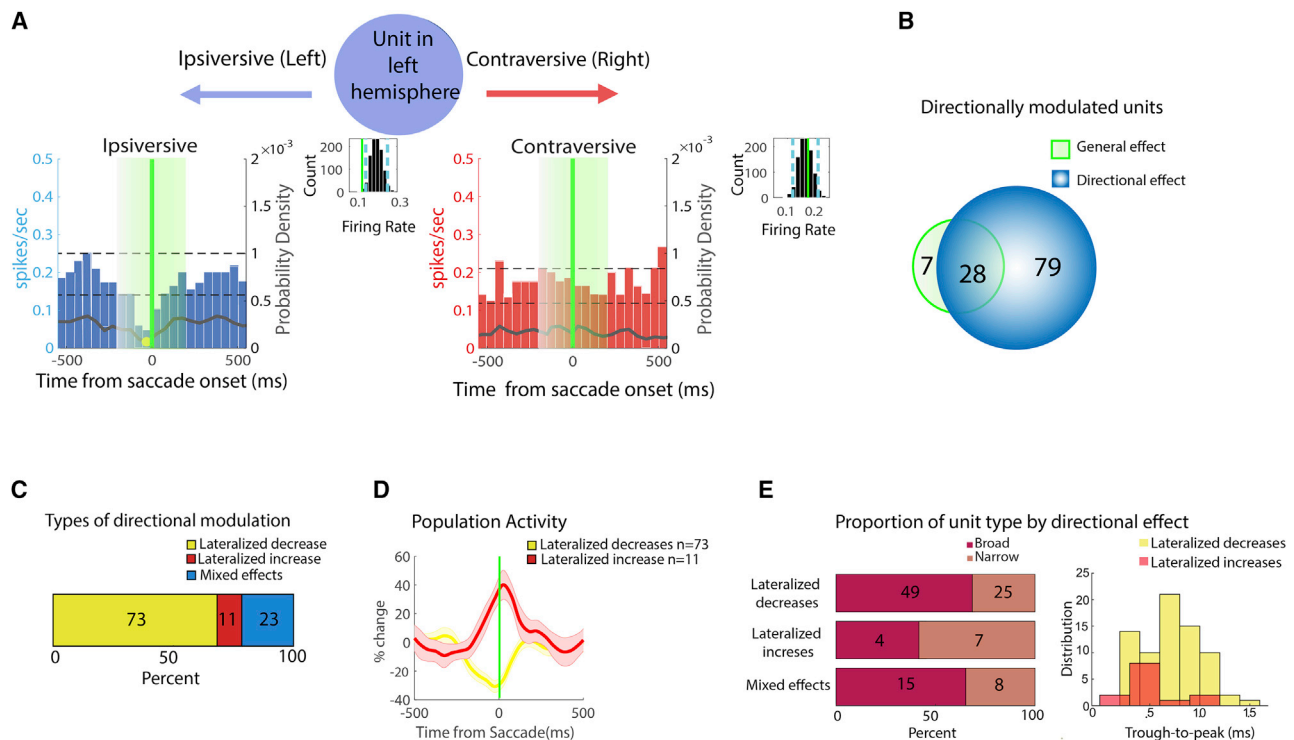


**Figure 3. Characteristics of directional modulation in the MTL**

(A) Ipsiversive and contraversive firing-rate changes of an example unit. Units were classified as “modulated by direction” if a significant increase or decrease was associated with contraversive or ipsiversive saccades. The unit in this example shows a decrease in ipsiversive saccades. Inset shows the distribution of units during control periods and mean firing rate during the saccadic period (green line).

(B) Venn diagram showing the proportion of units modulated by saccades (green) and the units that showed a directional effect (blue).

(C) Distribution of the different types of directional effects observed in the MTL.

(D) Population activity of neurons having decreasing or increasing effects showing that effects are aligned to saccade onset.

(E) Left: distribution of unit amplitudes (trough-to-peak) separated by directional effect observed in the MTL. Right: distribution of spike amplitude expressed by peak duration separated by neurons showing lateralized increases or decreases in firing rate.

See also [Figures S1](#) and [S2](#).

and increases did not differ from one another, firing-rate changes were confined to saccade onset ([Figure 3D](#)).

Firing-rate troughs and peaks in the occipital lobe occurred at  $-11 \pm 3.2$  ms and  $0.33 \pm 15.7$  ms relative to saccade onset. However, for units that demonstrated a rebound pattern, the rebound increase occurred at a longer latency ( $27 \pm 3$  ms; [Figure S2E](#)).

To explore the cell-type specificity of these firing-rate changes, we classified the units into two groups based on their waveform width: broad-spiking (putative pyramidal cells) and narrow-spiking (putative interneurons). Units that increased their firing rates in the peri-saccadic window were primarily narrow-spiking units (75%, 3/4) ([Figures S1E](#) and [S1F](#)). In contrast, among the more prevalent group with decreased firing rates, most neurons were broad spiking (74.1%,  $n = 23/31$ ). Likewise, most MTL neurons that presented lateralized decreases in firing were excitatory broad spiking (67.1%,  $n = 49/73$ ), whereas most

of the neurons that presented a lateralized increase in firing were inhibitory narrow spiking (63.6%,  $n = 7/11$ ). The majority of units displaying mixed directional effects were classified as broad spiking (65.21%,  $n = 15/23$ ) ([Figure 3E](#)). These findings suggest that saccades predominantly decrease the activity of putatively excitatory neurons and predominantly increase the activity of putatively inhibitory neurons.

Many neurons in occipital regions demonstrated a general decrease in the firing rate, like the modulated MTL neurons (43.64%,  $n = 24/55$ ). A large fraction, however, demonstrated a characteristic rebound activation pattern in the peri-saccadic window (56.36%,  $n = 31/55$ ), consisting of a transient decrease in firing in the peri-saccadic window, followed by a sharp increase ([Figure S2C](#)). Only a small subset of the modulated occipital lobe neurons demonstrated an increase in firing rate (5.45%,  $n = 3/55$ ) ([Figure S2D](#)). Akin to the modulated units in MTL

(C) Histogram of an example unit modulated by image onset noted by the increase in firing rate starting 500 ms after image onset (blue line). Inset shows the spike waveform and mean firing rate during the analysis period (200–1,700 ms).

(D) Top: distribution of units modulated by saccades. Bottom: proportion of units modulated (purple) by image onset.

(E) Venn diagram of visually modulated units (purple) or peri-saccadic period (green). No intersection was found between the two populations of units.

See also [Figures S1](#) and [S2](#) and [Table S1](#).

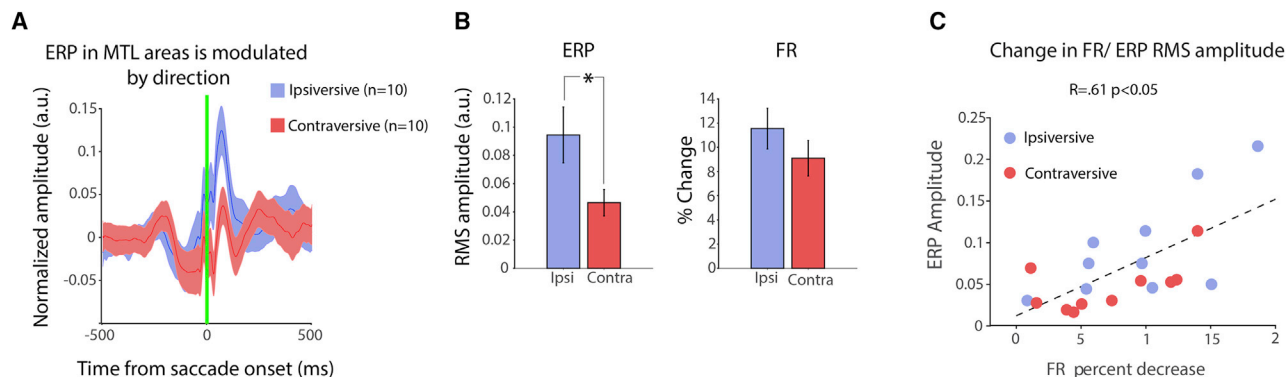


**Figure 4. Saccade-related neuronal activity and ERPs are directionally modulated and correlated to one another**

(A) ERP from electrodes localized in the MTL associated with ipsiversive and contraversive saccades.

(B) The left graph shows iEEG RMS amplitude separated by the direction of the saccade. RMS amplitudes of ipsiversive and contraversive ERPs are statistically significantly different (paired *t* test,  $p < 0.05$ ). The right graph shows the percentage modulation of units during the saccade period compared to randomized control periods.

(C) ERP RMS as function of FR decreases are positively correlated.

See also Figure S4.

structures, units in the occipital lobe that demonstrated firing-rate increases were mostly narrow spiking (66.7%,  $n = 2/3$ ). Interestingly, most rebound-modulated neurons in the occipital lobe were narrow spiking (80.64%,  $n = 25/31$ ; Figure S1F). As with the MTL, most occipital lobe neurons that decreased their firing rate were broad spiking (87.5%,  $n = 21/24$ ). Additionally, we investigated the directional modulation of units in the occipital lobe. Here, 62/125 (49.6%) units were directionally modulated. Unlike the MTL, there was a smaller overlap between the directionally modulated units and those units modulated when collapsing across saccade direction ( $n = 25$  units were common between both groups) (Figure S2I). Overall, there was significant directional modulation of single-unit activity in the occipital lobe, similar to that observed in the MTL.

We also explored saccade amplitude as a proxy for CD spatial information.<sup>42</sup> Supporting this approach, firing rate and saccade amplitude have been related in V1,<sup>54</sup> motor neurons in the brain stem,<sup>55,56</sup> and superior colliculus.<sup>57,58</sup> However, in humans using behavioral double saccade tasks, saccade amplitude was relevant for diagonal but not horizontal saccades,<sup>59</sup> which are a large portion of our distribution (Figure 1). Perhaps due to this limitation, we found only 23 of 524 units to have significant correlation with saccade amplitude, which was not significantly more than chance (binomial test). This suggests that saccade amplitude may not be transmitted to MTL structures; however, tasks specifically designed to address this are required to better address this question.

#### Saccade-related single-unit firing-rate decreases correlate to post-saccade ERP amplitude

Our previous work identified a short-latency, saccade onset aligned ERP in the MTL iEEG.<sup>15</sup> The combined observation that post-saccade ERPs align to saccade onset<sup>15</sup> and that single-unit firing-rate changes are confined to the peri-saccade interval suggests that the single-unit firing-rate changes may be correlated to ERP generation. If this is so, then the amplitude of the saccade-related ERP should depend on the saccade's direction and be correlated to single-unit firing-rate changes.

To explore these possibilities, we calculated the saccade-aligned ERP for both ipsiversive and contraversive saccades (Figure 4A). We found that the root mean squared (RMS) values 10–510 ms after saccade onset (corresponding to the significant portions of the saccade ERP from our previous work) depended on saccade direction (Figure 4B). Specifically, the ipsiversive saccade ERP had a significantly greater RMS magnitude than the contraversive ERP (ipsiversive =  $0.09 \pm 0.019$  normalized amplitude; contraversive =  $0.04 \pm 0.009$  normalized amplitude;  $p < 0.05$ ; Figure 4B). Although there were no significant differences for ipsiversive and contralateral saccades, more neurons were found to be modulated by direction than generally modulated, suggesting the importance of direction in the signal. This motivated an analysis of how directionally sensitive changes in firing rate relate to the amplitude of directionally modulated ERPs.

If the peri-saccadic firing-rate decreases underlie in some way the generation of the ERP, we would expect correlations between firing-rate changes and ERP amplitude. To explore this, we measured firing-rate decreases in the directionally modulated MTL units (contraversive or ipsiversive modulated unit) and corresponding ERP (contraversive or ipsiversive ERP from electrode corresponding to the modulated unit) RMS amplitude for each patient. One patient was eliminated from this analysis as no modulated units were found. Spearman's rank correlation between these measures revealed that firing-rate decreases were positively correlated to ERP magnitude (Figure 4C). Thus, the more strongly BS neurons were inhibited—the cell type that demonstrates the most consistent decrease in firing rate—the larger the ERP. We infer from this relationship that the post-saccade ERP<sup>15</sup> may be a proxy for the strength of an inhibitory modulating signal (see discussion).

#### DISCUSSION

In our previous work,<sup>15</sup> we presented iEEG evidence that the MTL is uniquely modulated around the time of saccades as



compared to image onset, and the alignment to saccade onset was suggestive of a CD-like signal. These conclusions comported well with extensive NHP literature regarding the extra-retinal contributions to the modulation of LFPs in MTL and other visual areas.<sup>13,14,20,41,50,60,61</sup> Here, we present six key findings derived from human single-unit recordings that greatly extend these findings to provide a plausible mechanism by which extra-retinal signals accompanying saccades modulate the hippocampus and surrounding MTL structures in humans. Our six key findings are that (1) the peri-saccade interval is dominated by inhibition (firing-rate decreases of BS units, firing-rate increases of NS units), (2) single-unit activity is modulated largely before and during the saccade, (3) the modulation contained directional information, (4) distinct population of neurons are modulated by saccade and image onset, (5) saccadic modulation of occipital neuronal activity is distinct from MTL neuronal activity modulation, and (6) the amplitude of the post-saccade ERP is correlated to the magnitude of the firing-rate decrease of BS units in the peri-saccadic interval. Through the manuscript, we grouped MTL results because constituent regions showed similar modulation patterns (Figure S3), suggesting a CD-like signal is widely present within the MTL and, thus, likely generally relevant to mnemonic processes, albeit through the variable roles served by the different structures.<sup>62</sup> However, given that the majority of units we observed within the MTL were from the hippocampus and the extensive knowledge about hippocampal physiology and function, we focus our discussion specifically on hippocampal circuitry as an exemplar.

#### Firing-rate decreases dominate the peri-saccade period

The combination of increased NS and decreased BS firing rates suggests that the incoming saccade-related signal has a net inhibitory influence. This pattern is consistent with a general CD motif, in which motor-related signals excite local inhibitory interneurons, which then inhibit excitatory neurons.<sup>16,17</sup> There are other possibilities. It could be argued that decreases in BS activity arise from the reductions in afferent visual input during saccadic suppression.<sup>25</sup> Arguing against this possibility, however, BS firing rates change before afferent visual input would arrive in the MTL.<sup>45,63</sup> Moreover, the accompanying increases in NS unit activity would be hard to explain with decreased afferent drive. Another possibility is direct inhibition through long-range GABAergic projections. However, the direction of the neuronal activity modulation we observe makes this unlikely.<sup>64</sup>

Beyond eye movements, such an inhibition governed hippocampal modulation is well described in response to both alerting stimuli in rodents (auditory clicks, smell, touching)<sup>65–67</sup> and electrical stimulation of intrahippocampal pathways.<sup>68–70</sup> Considering these parallels, perhaps eye-movement plans act as an alerting signal, preparing the hippocampus for important new visual input. Indeed, hippocampal phase modulation temporally organizes LTP and LTD periods relative to the stimulus.<sup>71</sup> Thus, saccades and a myriad of externally driven salience signals may leverage a general mechanism—inhibition mediated modulation—to organize the encoding of new and important information. This link between active visual sensing and specific memory processes in mnemonic structures is consistent with an extensive literature rife with evidence linking saccadic eye

movements to memory strength (for review, see Meister and Bufalo,<sup>8</sup> Hannula et al.,<sup>72</sup> and Ryan et al.<sup>73</sup>).

Although we invoke an inhibitory CD circuit motif to explain the observed firing-rate changes, predictive attentional updating<sup>74</sup> has been proposed as a competing/complementary mechanism to predictive remapping mediated by a CD.<sup>32,51</sup> Interestingly attentional mechanisms are also accompanied by increased interneuronal activity evidenced as either increased firing rates of narrow-spiking units<sup>75</sup> or increases in gamma band coherence<sup>76</sup> that reflect increased spiking of parvalbumin positive interneurons.<sup>77,78</sup> It is thus possible that the increased firing rates of narrow-spiking units we observe is a manifestation of attentional updating.<sup>74</sup> Unfortunately, our study does not allow the teasing apart of how attention and visual motor commands interact, albeit representing an exciting avenue of research into two processes that are both intimately related to mnemonic processing. Of note, the amplitude of the pre-potential from –100 to 0 ms did not correlate with the firing rate (Figure S4). If this pre-potential represents some form of motor planning/attentional updating<sup>74</sup> signal, it does not seem to be correlated with firing-rate changes.

#### Single-unit activity reflects the early arrival of spatial and temporal parameters of ensuing eye movement

Our finding that MTL single units were predominantly modulated in the pre-saccadic window comports well with our previous observation that MTL iEEG modulation is aligned to saccade onset and not its termination (i.e., fixation).<sup>15</sup> Both findings are consistent with the notion that MTL neurons are likely modulated by the motor planning of saccades rather than the resulting change in visual input. We also found strong directional modulation in MTL neuronal activity, with a vast majority of single units showing directional modulation (107/114, 93.9%). Although directionally modulated units were also present in the occipital lobe, they represented a relatively smaller proportion of the total number of modulated occipital units (62/87, 71%). It has been suggested that the modulation of units directly receiving visual information reflects an exafference signal more than the CD signal.<sup>28</sup> Accordingly, the firing-rate changes we observe in MTL units may reflect the effects of a less adulterated CD, whereas the occipital lobe saccade modulation is likely the summed influence of a CD and visual reafference.<sup>41</sup>

#### Role of directional information in the MTL

How might a CD signal be utilized in the MTL? Rather than indiscriminately inhibiting BS units, our results suggest that the CD could inhibit (or excite) distinct MTL units depending on the associated saccade's direction. This spatial tuning is reminiscent of the spatial and directional information that MTL structures in rodents use to create maps of the physical world or cognitive maps more generally;<sup>79,80</sup> place cells,<sup>79</sup> grid cells,<sup>81,82</sup> and head direction cells<sup>83</sup> have been demonstrated in the MTL. Primates, by contrast, primarily explore their physical world with their eyes. It is thus unsurprising that spatial information about eye movements should be reflected in primate MTL neuronal activity.<sup>14,18,53,84</sup>

Here, we add to this literature by showing that this directionally tuned peri-saccadic modulation is primarily inhibitory, suggesting that its role may be akin to the well-accepted role of

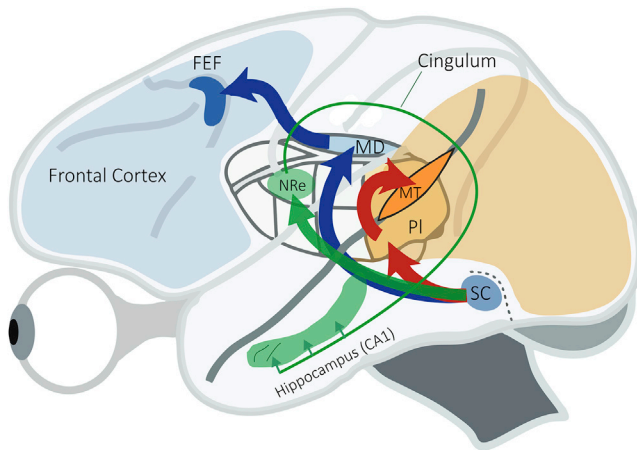


**Figure 5. Proposed pathway involving the MTL in saccadic eye movements**

Modified figure from Berman et al.,<sup>24</sup> which is itself a summary of Sommer and Wurtz,<sup>21</sup> to include the novel pathway proposed here (green) from SC to nucleus reuniens (NRe) of the thalamus to area CA1 of the hippocampus. Red (SC → PI → MT) and blue (SC → MD → FEF) pathways have been well described. FEF, frontal eye field; SC, superior colliculus; MD, medial dorsal nucleus; PI, pulvinar; MT, area MT.

CDs in stabilizing visual perception.<sup>21,32,85</sup> Specifically, CDs are thought to “unite separate retinal images into a stable visual scene,” as was beautifully demonstrated in experiments that inactivate the CD while NHP explore visual scenes.<sup>32</sup> The resulting alterations of visual perception provided early links between CD and perception. The neuronal mechanism underlying such a perceptual role for a CD was speculated to be akin to the anticipatory shifting of receptive fields in the lateral intraparietal sulcus during saccadic eye movements.<sup>51</sup> Analogously, the directional information (i.e., the “path” in path integration) we identify in the human hippocampus could be used to stitch together sequentially sampled windows into a singular memory of a scene.<sup>6,7,86</sup> Perhaps this mechanism may even generalize to reflect the hippocampus’ emerging role in encoding “conceptual maps.”<sup>80,87</sup> Whether initiated by the traversal of visual or conceptual space, a CD carrying directional information could facilitate a construction from parts, reminiscent of episodic memory semanticization,<sup>87</sup> through path integration.

### Putative CD circuit

Our evidence supporting CD-mediated modulation of MTL single units comports well with extensive literature regarding the extra-retinal modulation of LFPs in MTL and other visual areas.<sup>13,14,20,41,50,60,61</sup> Circuits proposed for these brain regions include (1) the pathway from the superior colliculus to the medial dorsal nucleus to frontal eye fields for receptive field remapping<sup>52</sup> and (2) a saccadic suppression pathway from superior colliculus to pulvinar to middle temporal cortex, which may function to maintain stable visual percepts (Figure 5). For both these motifs, the thalamus is a common relay between superior colliculus and cortical regions, but to our knowledge, there is no currently described pathway from superior colliculus to hippocampus. It is thus possible that the hippocampus inherits the effects of a CD from other brain regions. Indeed, saccades

have been shown to be accompanied by modulation of neural activity in low-level visual areas such as the lateral geniculate nucleus,<sup>88</sup> V1,<sup>29,41,50</sup> and V4,<sup>89</sup> which ultimately project to the hippocampus via the dorsal stream. However, it should be noted that we and others observed firing-rate increases in early visual areas later than saccade-related changes in the MTL,<sup>50</sup> making it unlikely that the firing-rate modulation we observe before and during the saccade in the MTL is relayed from other cortical areas.

Alternatively, we propose a speculative circuit that is homologous to known CD circuits within the visual system (Figure 5). It potentially explains (1) how the output from the superior colliculus arrives in the hippocampus, (2) how the ERP is generated and the expected firing changes in different cell types, (3) how a CD arising from the superior colliculus could uniquely mediate its effects through inhibition within the hippocampus, and (4) why units that are modulated by saccades are different from those modulated by image onset.

The nucleus reuniens (Figure 5; adapted from Berman et al.<sup>24</sup>) is a midline thalamic relay nucleus<sup>90</sup> with direct input to the hippocampus, where it synapses exclusively on inhibitory interneurons in the CA1 region.<sup>91,92</sup> Requiring experimental evidence, reuniens’ role in mediating a CD from superior colliculus to the hippocampus is well supported by anatomical and functional data. Specifically, (1) superior colliculus motor neurons have direct projections to reuniens,<sup>93,94</sup> (2) reuniens stimulation can drive CA1 interneurons to threshold and not pyramidal cells;<sup>92,95,96</sup> (3) reuniens axons synapse exclusively on NGF interneurons, and thus reuniens exerts its effects primarily via inhibition;<sup>91,92</sup> and (4) reuniens has directional information<sup>97</sup> that is likely transmitted to the hippocampus and entorhinal cortices.<sup>92,98</sup> This circuit motif thus potentially explains the dichotomy that we see between units that are modulated with saccades and units that are modulated by image onset since the reuniens pathway is highly specific for interneurons. However, additional empirical investigations are required to substantiate this proposal, ideally including causal manipulations to these candidate pathways that are not feasible to perform in humans.

Furthermore, in the context of this putative circuit (Figure 5), we propose that the saccade-related ERP is generated by both post-synaptic potentials generated in interneurons<sup>99</sup> and the subsequent alteration of the phase of ongoing spiking through a pause-rebound mechanism.<sup>100</sup> This would be analogous to how brief stimulation of the perforant path yields a lasting firing-rate modulation at theta frequency via inhibition.<sup>68</sup> Notably, the saccade-related ERP we observed need not reflect the modulation of ongoing oscillations. This is an important consideration, since continuous oscillations like theta are not prominent in the primate hippocampus<sup>101–103</sup> and are certainly not continuous like those in the rodent.<sup>104</sup> Nonetheless, it is still possible that a theta phase reset is a mechanism by which a CD operates.<sup>15,105,106</sup> However, here, we delve deeper, specifically into a potential circuit that might underlie the results we observe. This circuit also potentially explains the correlation between single-unit inhibition and ERP amplitude (Figure 4C), since both signals would be related to the magnitude of PSPs in interneurons and, consequently, the increased probability of consistently timed rebound spikes.<sup>100</sup>

### Limitations of study

Given that our work was in humans, we could not perturb nodes of the proposed CD circuit, a critical step in determining if a CD causally drives firing-rate modulations we observe in the MTL. Despite this limitation, we believe our findings can serve as a basis for work where such investigations are undertaken, as has been done for other CD circuits.<sup>24</sup>

If the peri-saccade modulation is solely a result of extra-retinal signals, it should persist in darkness. Although the restrictions of our clinical setting precluded our test of this hypothesis, previous work with human and NHPs suggests that both saccade-related ERPs and neuronal activity modulation are observed in darkness and/or blank screens<sup>18–20,60</sup> (but see Hoffman et al.<sup>14</sup>). For example, in humans, rapid eye movements in sleep and wakefulness generated both ERPs and neuronal activity modulations in the peri-saccadic period. The pattern was also characteristic of decreases in single-unit firing rates before the rapid eye movement with increases afterward in all cases other than awake non-visual stimulation.<sup>20</sup> Their observed rebound pattern is reminiscent of the firing-rate change observed exclusively in occipital lobe units (Figure 1), a result that might have arisen from averaging of up- and down-modulated units.

By contrast, a recent NHP study demonstrated no appreciable modulation in hippocampal population activity following saccades on a blank background, despite saccade-associated phase clustering in the iEEG.<sup>60</sup> However, this analysis approach averaged across all units, rather than focusing on the small proportion of modulated units, as we and others have done. Had this more sensitive approach been used, neuronal activity modulation may have been observed while looking at a blank screen. Relatedly, our initial investigations only revealed phase clustering when exploring images, not during saccades on a dark screen.<sup>14</sup> However, this lack of clustering was based on saccades made during a blank screen in the inter-trial interval immediately following reward delivery, rather than longer periods of complete darkness outside the task regime. Also only iEEG data were analyzed without single-unit activity, and the analysis was from data collected from a single NHP. Thus, although there is some heterogeneity in the literature, a large body of work supports the hypothesis that saccadic modulation of activity in the MTL persists in the absence of visual input, further supporting the notion that this type of modulation arises from an extra-retinal signal.

### Conclusion

In summary, we characterize neuronal activity in MTL and occipital lobe structures to explore the hypothesis that a saccade-related CD-like signal exists in mnemonic structures of the human brain. Employing a unit-by-unit analysis of firing-rate changes, we provide evidence that saccades are associated with a modulating influence characterized largely by inhibition and containing directional information. We show that saccade-related modulation is more inhibitory and directionally tuned in the MTL than in the occipital lobe units. All these distinctions are consistent with MTL neurons receiving a saccade-related CD signal. We additionally propose a novel circuit underlying our findings where the nucleus reuniens of the thalamus—a key hub for memory processes<sup>90,95,107–109</sup>—plays a central

role in transmitting the output from motor layers of the superior colliculus<sup>93,94,110</sup> to the MTL.

### STAR★METHODS

Detailed methods are provided in the online version of this paper and include the following:

- KEY RESOURCES TABLE
- RESOURCE AVAILABILITY
  - Lead contact
  - Materials availability
  - Data and code availability
- EXPERIMENTAL MODEL AND SUBJECT DETAILS
- METHOD DETAILS
  - Experimental design
  - Electrophysiology
  - Analysis of eye-tracking data
- QUANTIFICATION AND STATISTICAL ANALYSIS
  - Analysis of electrophysiological data

### SUPPLEMENTAL INFORMATION

Supplemental information can be found online at <https://doi.org/10.1016/j.cub.2022.06.015>.

### ACKNOWLEDGMENTS

We thank Ivan Soltesz and Alexandra Pierri Chatzikalymniou for insightful discussions about hippocampal CA1 electrophysiology. We would like to acknowledge Azadeh Naderian and Harish Babu, who helped with some of the initial sorting of the single units.

### AUTHOR CONTRIBUTIONS

Conceptualization, C.N.K. and T.A.V.; methodology, K.P., C.N.K., K.D.D., and A.G.P.S.; software, C.N.K., K.P., and A.G.P.S.; formal analysis, A.G.P.S., K.P., and C.N.K.; investigation, C.N.K., A.G.P.S., and K.P.; data collection, C.N.K., A.G.P.S., K.P., and V.B.; single-unit selection, A.G.P.S.; visualization, A.G.P.S., K.P., and C.N.K.; writing – original draft, C.N.K., A.G.P.S., and K.P.; writing – review & editing, C.N.K., A.G.P.S., K.P., K.L.H., K.D.D., and T.A.V.; surgical implantation, S.K.K. and T.A.V.; funding acquisition, T.A.V.; resources, T.A.V.; supervision, T.A.V.

### DECLARATION OF INTERESTS

T.A.V. is an investor in the company Neurescence, which has no involvement in this study. T.A.V. provides consulting to the company Panaxium, which has no involvement in this study. C.N.K. and K.P. provide consulting to Novela Neurotech, which has no involvement in this study.

Received: August 11, 2021

Revised: April 4, 2022

Accepted: June 8, 2022

Published: July 1, 2022

### REFERENCES

1. Rolls, E.T., and Wirth, S. (2018). Spatial representations in the primate hippocampus, and their functions in memory and navigation. *Prog. Neurobiol.* 177, 90–113.
2. Ekstrom, A.D. (2015). Why vision is important to how we navigate. *Hippocampus* 25, 731–735.

3. Schroeder, C.E., Wilson, D.A., Radman, T., Scharfman, H.E., and Lakatos, P. (2010). Dynamics of active sensing and perceptual selection. *Curr. Opin. Neurobiol.* *20*, 172–176.
4. Troncoso, X.G., Otero-Millan, J., Macknik, S.L., Serrano-Pedraza, I., Martinez-Conde, S., Troncoso, X.G., Macknik, S.L., Serrano-Pedraza, I., and Martinez-Conde, S. (2008). Saccades and microsaccades during visual fixation, exploration, and search: foundations for a common saccadic generator. *J. Vis.* *9*, 447.
5. Chau, V.L., Murphy, E.F., Rosenbaum, R.S., Ryan, J.D., and Hoffman, K.L. (2011). A flicker change detection task reveals object-in-scene memory across species. *Front. Behav. Neurosci.* *5*, 58.
6. Yoo, S.A., Rosenbaum, R.S., Tsotsos, J.K., Fallah, M., and Hoffman, K.L. (2020). Long-term memory and hippocampal function support predictive gaze control during goal-directed search. *J. Vis.* *20*, 10.
7. Wynn, J.S., Bone, M.B., Dragan, M.C., Hoffman, K.L., Buchsbaum, B.R., and Ryan, J.D. (2016). Selective scanpath repetition during memory-guided visual search. *Vis. Cogn.* *24*, 15–37.
8. Meister, M.L.R.R., and Buffalo, E.A. (2016). Getting directions from the hippocampus: the neural connection between looking and memory. *Neurobiol. Learn. Mem.* *134*, 135–144.
9. Kafkas, A., and Montaldi, D. (2011). Recognition memory strength is predicted by pupillary responses at encoding while fixation patterns distinguish recollection from familiarity. *Q. J. Exp. Psychol. (Hove)* *64*, 1971–1989.
10. Liu, Z.-X., Shen, K., Olsen, R.K., and Ryan, J.D. (2017). Visual sampling predicts hippocampal activity. *J. Neurosci.* *37*, 599–609.
11. Olsen, R.K., Chiew, M., Buchsbaum, B.R., and Ryan, J.D. (2014). The relationship between delay period eye movements and visuospatial memory. *J. Vis.* *14*, 1–11.
12. Shen, K., Bezgin, G., Selvam, R., McIntosh, A.R., and Ryan, J.D. (2016). An anatomical interface between memory and oculomotor systems. *J. Cogn. Neurosci.* *28*, 1772–1783.
13. Jutras, M.J., Fries, P., and Buffalo, E.A. (2013). Oscillatory activity in the monkey hippocampus during visual exploration and memory formation. *Proc. Natl. Acad. Sci. USA* *110*, 13144–13149.
14. Hoffman, K.L., Dragan, M.C., Leonard, T.K., Micheli, C., Montefusco-Siegmund, R., and Valiante, T.A. (2013). Saccades during visual exploration align hippocampal 3–8 Hz rhythms in human and non-human primates. *Front. Syst. Neurosci.* *7*, 43.
15. Katz, C.N., Patel, K., Talakoub, O., Groppe, D., Hoffman, K.L., and Valiante, T.A. (2020). Differential generation of saccade, fixation, and image-onset event-related potentials in the human mesial temporal lobe. *Cereb. Cortex* *30*, 5502–5516.
16. Crapse, T.B., and Sommer, M.A. (2008). Corollary discharge circuits in the primate brain. *Curr. Opin. Neurobiol.* *18*, 552–557.
17. Crapse, T.B., and Sommer, M.A. (2008). Corollary discharge across the animal kingdom. *Nat. Rev. Neurosci.* *9*, 587–600.
18. Ringo, J.L., Sobotka, S., Diltz, M.D., and Bunce, C.M. (1994). Eye movements modulate activity in hippocampal, parahippocampal, and inferotemporal neurons. *J. Neurophysiol.* *71*, 1285–1288.
19. Sobotka, S., and Ringo, J.L. (1997). Saccadic eye movements, even in darkness, generate event-related potentials recorded in medial sputum and medial temporal cortex. *Brain Res.* *756*, 168–173.
20. Andriillon, T., Nir, Y., Cirelli, C., Tononi, G., and Fried, I. (2015). Single-neuron activity and eye movements during human REM sleep and awake vision. *Nat. Commun.* *6*, 7884.
21. Sommer, M.A., and Wurtz, R.H. (2008). Brain circuits for the internal monitoring of movements. *Annu. Rev. Neurosci.* *31*, 317–338.
22. Richmond, B.J., and Wurtz, R.H. (1980). Vision during saccadic eye movements. II. A corollary discharge to monkey superior colliculus. *J. Neurophysiol.* *43*, 1156–1167.
23. Robinson, D.L., and Wurtz, R.H. (1976). Use of an extraretinal signal by monkey superior colliculus neurons to distinguish real from self-induced stimulus movement. *J. Neurophysiol.* *39*, 852–870.
24. Berman, R.A., Cavanaugh, J., McAlonan, K., and Wurtz, R.H. (2017). A circuit for saccadic suppression in the primate brain. *J. Neurophysiol.* *117*, 1720–1735.
25. Idrees, S., Baumann, M.P., Franke, F., Münch, T.A., and Hafed, Z.M. (2020). Perceptual saccadic suppression starts in the retina. *Nat. Commun.* *11*, 1977.
26. Deubel, H., Schneider, W.X., and Bridgeman, B. (1996). Postsaccadic target blanking prevents saccadic suppression of image displacement. *Vision Res.* *36*, 985–996.
27. Deubel, H., Bridgeman, B., and Schneider, W.X. (2004). Different effects of eyelid blinks and target blanking on saccadic suppression of displacement. *Percept. Psychophys.* *66*, 772–778.
28. Rajkai, C., Lakatos, P., Chen, C.M., Pincze, Z., Karmos, G., and Schroeder, C.E. (2008). Transient cortical excitation at the onset of visual fixation. *Cereb. Cortex* *18*, 200–209.
29. Barczak, A., Haegens, S., Ross, D.A., McGinnis, T., Lakatos, P., and Schroeder, C.E. (2019). Dynamic modulation of cortical excitability during visual active sensing. *Cell Rep.* *27*, 3447–3459.e3.
30. Concha-Miranda, M., Ríos, J., Bou, J., Valdes, J.L., and Maldonado, P.E. (2019). Timing is of the essence: improvement in perception during active sensing. *Front. Behav. Neurosci.* *13*, 96.
31. Wurtz, R.H. (2018). Corollary discharge contributions to perceptual continuity Across saccades. *Annu. Rev. Vis. Sci.* *4*, 215–237.
32. Cavanaugh, J., Berman, R.A., Joiner, W.M., and Wurtz, R.H. (2016). Saccadic corollary discharge underlies stable visual perception. *J. Neurosci.* *36*, 31–42.
33. Malassisi, R., Del Cul, A., and Collins, T. (2015). Corollary discharge failure in an oculomotor task is related to delusional ideation in healthy Individuals. *PLoS One* *10*, e0134483.
34. Thakkar, K.N., Schall, J.D., Heckers, S., and Park, S. (2015). Disrupted saccadic corollary discharge in schizophrenia. *J. Neurosci.* *35*, 9935–9945.
35. Pack, C.C. (2014). Eye movements as a probe of corollary discharge function in schizophrenia. *ACS Chem. Neurosci.* *5*, 326–328.
36. Heinks-Maldonado, T.H., Mathalon, D.H., Houde, J.F., Gray, M., Faustman, W.O., and Ford, J.M. (2007). Relationship of imprecise corollary discharge in schizophrenia to auditory hallucinations. *Arch. Gen. Psychiatry* *64*, 286–296.
37. Railo, H., Olkonieni, H., Eeronheimo, E., Pääkkönen, O., Joutsa, J., and Kaasinen, V. (2018). Dopamine and eye movement control in Parkinson's disease: deficits in corollary discharge signals? *PeerJ* *6*, e6038.
38. Riek, H., Coe, B., Brien, D., Black, S., Borrie, M., Dowlatshahi, D., Finger, E., Freedman, M., Kwan, D., Lang, A., et al. (2020). Saccadic behaviour in an eye-tracking task is differentially altered by neurodegenerative diseases. *Neurology* *94*, 2184.
39. Peltsch, A., Hemraj, A., Garcia, A., and Munoz, D.P. (2014). Saccade deficits in amnesic mild cognitive impairment resemble mild Alzheimer's disease. *Eur. J. Neurosci.* *39*, 2000–2013.
40. Wang, J., Guo, X., Zhuang, X., Chen, T., and Yan, W. (2017). Disrupted pursuit compensation during self-motion perception in early Alzheimer's disease. *Sci. Rep.* *7*, 4049.
41. Purpura, K.P., Kalik, S.F., and Schiff, N.D. (2003). Analysis of perisaccadic field potentials in the occipitotemporal pathway during active vision. *J. Neurophysiol.* *90*, 3455–3478.
42. Wurtz, R.H., and Sommer, M.A. (2004). Identifying corollary discharges for movement in the primate brain. *Prog. Brain Res.* *144*, 47–60.
43. Sommer, M.A., and Wurtz, R.H. (2002). A pathway in primate brain for internal monitoring of movements. *Science* *296*, 1480–1482.
44. Kornblith, S., Quiroga, R.Q., Koch, C., Fried, I., Mormann, F., Kornblith, S., Quiroga, R.Q., Koch, C., Fried, I., and Mormann, F. (2017). Persistent single-neuron activity during working memory in the human medial temporal lobe. *Curr. Biol.* *27*, 1026–1032.

45. Mormann, F., Kornblith, S., Quiroga, R.Q., Kraskov, A., Cerf, M., Fried, I., and Koch, C. (2008). Latency and selectivity of single neurons indicate hierarchical processing in the human medial temporal lobe. *J. Neurosci.* *28*, 8865–8872.
46. Quiroga, R.Q., Reddy, L., Kreiman, G., Koch, C., and Fried, I. (2005). Invariant visual representation by single neurons in the human brain. *Nature* *435*, 1102–1107.
47. Mormann, F., Kornblith, S., Cerf, M., Ison, M.J., Kraskov, A., Tran, M., Knieling, S., Quian Quiroga, R., Koch, C., and Fried, I. (2017). Scene-selective coding by single neurons in the human parahippocampal cortex. *Proc. Natl. Acad. Sci. USA* *114*, 1153–1158.
48. Faraut, M.C.M., Carlson, A.A., Sullivan, S., Tudusciuc, O., Ross, I., Reed, C.M., Chung, J.M., Mamelak, A.N., and Rutishauser, U. (2018). Dataset of human medial temporal lobe single neuron activity during declarative memory encoding and recognition. *Sci. Data* *5*, 180010.
49. Rutishauser, U., Ye, S., Koroma, M., Tudusciuc, O., Ross, I.B., Chung, J.M., and Mamelak, A.N. (2015). Representation of retrieval confidence by single neurons in the human medial temporal lobe. *Nat. Neurosci.* *18*, 1041–1050.
50. Ito, J., Maldonado, P., Singer, W., Grun, S., and Grün, S. (2011). Saccade-related modulations of neuronal excitability support synchrony of visually elicited spikes. *Cereb. Cortex* *21*, 2482–2497.
51. Duhamel, J.-R.R., Colby, C.L., and Goldberg, M.E. (1992). The updating of the representation of visual space in parietal cortex by intended eye movements. *Science* *255*, 90–92.
52. Sommer, M.A., and Wurtz, R.H. (2006). Influence of the thalamus on spatial visual processing in frontal cortex. *Nature* *444*, 374–377.
53. Killian, N.J., Potter, S.M., and Buffalo, E.A. (2015). Saccade direction encoding in the primate entorhinal cortex during visual exploration. *Proc. Natl. Acad. Sci. USA* *112*, 15743–15748.
54. Snodderly, D.M. (2016). A physiological perspective on fixational eye movements. *Vision Res.* *118*, 31–47.
55. Ling, L., Fuchs, A.F., Phillips, J.O., and Freedman, E.G. (1999). Apparent dissociation between saccadic eye movements and the firing patterns of premotor neurons and motoneurons. *J. Neurophysiol.* *82*, 2808–2811.
56. Vasudevan, V., Padhi, R., and Murthy, A. (2016). Characterization of pulse-step input for saccadic eye movements. In 2016 Indian Control Conf. ICC 2016—Proc., pp. 13–18.
57. Goossens, H.H.L.M., and van Opstal, A.J. (2012). Optimal control of saccades by spatial-temporal activity patterns in the monkey superior colliculus. *PLoS Comput. Biol.* *8*, e1002508.
58. Groh, J.M. (2011). Effects of initial eye position on saccades evoked by microstimulation in the primate superior colliculus: implications for models of the SC read-out process. *Front. Integr. Neurosci.* *4*, 130.
59. Joiner, W.M. (2010). Amplitudes and directions of individual saccades can be adjusted by corollary discharge. *J. Vis.* *10*, 1–12.
60. Doucet, G., Gulli, R.A., Corrigan, B.W., Duong, L.R., and Martinez-Trujillo, J.C. (2019). Modulation of local field potentials and neuronal activity in primate hippocampus during saccades. *Hippocampus* *30*, 1–18.
61. Bartlett, A.M., Ovaysikia, S., Logothetis, N.K., and Hoffman, K.L. (2011). Saccades during object viewing modulate oscillatory phase in the superior temporal sulcus. *J. Neurosci.* *31*, 18423–18432.
62. LaBar, K.S., and Cabeza, R. (2006). Cognitive neuroscience of emotional memory. *Nat. Rev. Neurosci.* *7*, 54–64.
63. Schmolesky, M.T., Wang, Y., Hanes, D.P., Thompson, K.G., Leutgeb, S., Schall, J.D., and Leventhal, A.G. (1998). Signal timing across the macaque visual system. *J. Neurophysiol.* *79*, 3272–3278.
64. Caputi, A., Melzer, S., Michael, M., and Monyer, H. (2013). The long and short of GABAergic neurons. *Curr. Opin. Neurobiol.* *23*, 179–186.
65. Green, J.D., and Arduini, A.A. (1954). Hippocampal electrical activity in arousal. *J. Neurophysiol.* *17*, 533–557.
66. Vinogradova, O.S.S. (1995). Expression, control, and probable functional significance of the neuronal theta-rhythm. *Prog. Neurobiol.* *45*, 523–583.
67. Givens, B. (1996). Stimulus-evoked resetting of the dentate theta rhythm: relation to working memory. *NeuroReport* *8*, 159–163.
68. Zugaro, M.B., Monconduit, L., and Buzsáki, G. (2005). Spike phase precession persists after transient intrahippocampal perturbation. *Nat. Neurosci.* *8*, 67–71.
69. Williams, J.M., and Givens, B. (2003). Stimulation-induced reset of hippocampal theta in the freely performing rat. *Hippocampus* *13*, 109–116.
70. Buño, W., Garcia-Sanchez, J.L., and Garcia-Austt, E. (1978). Reset of hippocampal rhythmical activities by afferent stimulation. *Brain Res. Bull.* *3*, 21–28.
71. McCartney, H., Johnson, A.D., Weil, Z.M., and Givens, B. (2004). Theta reset produces optimal conditions for long-term potentiation. *Hippocampus* *14*, 684–687.
72. Hannula, D.E., Althoff, R.R., Warren, D.E., Riggs, L., Cohen, N.J., and Ryan, J.D. (2010). Worth a glance: using eye movements to investigate the cognitive neuroscience of memory. *Front. Hum. Neurosci.* *4*, 166.
73. Ryan, J.D., Shen, K., and Liu, Z.X. (2020). The intersection between the oculomotor and hippocampal memory systems: empirical developments and clinical implications. *Ann. N. Y. Acad. Sci.* *1464*, 115–141.
74. Wilmott, J.P., and Michel, M.M. (2021). Transsaccadic integration of visual information is predictive, attention-based, and spatially precise. *J. Vis.* *21*, 14.
75. Mitchell, J.F., Sundberg, K.A., and Reynolds, J.H. (2007). Differential attention-dependent response modulation across cell classes in macaque visual area V4. *Neuron* *55*, 131–141.
76. Gregoriou, G.G., Gots, S.J., Zhou, H., and Desimone, R. (2009). High-frequency, long-range coupling between prefrontal and visual cortex during attention. *Science* *324*, 1207–1210.
77. Sohal, V.S., Zhang, F., Yizhar, O., and Deisseroth, K. (2009). Parvalbumin neurons and gamma rhythms enhance cortical circuit performance. *Nature* *459*, 698–702.
78. Cardin, J.A., Carlén, M., Meletis, K., Knoblich, U., Zhang, F., Deisseroth, K., Tsai, L.H., and Moore, C.I. (2009). Driving fast-spiking cells induces gamma rhythm and controls sensory responses. *Nature* *459*, 663–667.
79. O’Keefe, J., and Dostrovsky, J. (1971). The hippocampus as a spatial map. Preliminary evidence from unit activity in the freely-moving rat. *Brain Res.* *34*, 171–175.
80. Epstein, R.A., Patai, E.Z., Julian, J.B., and Spiers, H.J. (2017). The cognitive map in humans: spatial navigation and beyond. *Nat. Neurosci.* *20*, 1504–1513.
81. Hafting, T., Fyhn, M., Molden, S., Moser, M.-B., and Moser, E.I. (2005). Microstructure of a spatial map in the entorhinal cortex. *Nature* *436*, 801–806.
82. Jacobs, J., Weidemann, C.T., Miller, J.F., Solway, A., Burke, J.F., Wei, X.X., Suthana, N., Sperling, M.R., Sharan, A.D., Fried, I., and Kahana, M.J. (2013). Direct recordings of grid-like neuronal activity in human spatial navigation. *Nat. Neurosci.* *16*, 1188–1190.
83. Sargolini, F., Fyhn, M., Hafting, T., McNaughton, B.L., Witter, M.P., Moser, M.B., and Moser, E.I. (2006). Conjunctive representation of position, direction, and velocity in entorhinal cortex. *Science* *312*, 758–762.
84. Killian, N.J., Jutras, M.J., and Buffalo, E.A. (2012). A map of visual space in the primate entorhinal cortex. *Nature* *491*, 761–764.
85. Joiner, W.M., Cavanaugh, J., FitzGibbon, E.J., and Wurtz, R.H. (2013). Corollary discharge contributes to perceived eye location in monkeys. *J. Neurophysiol.* *110*, 2402–2413.
86. Wynn, J.S., Ryan, J.D., and Buchsbaum, B.R. (2020). Eye movements support behavioral pattern completion. *Proc. Natl. Acad. Sci. USA* *117*, 6246–6254.
87. Buzsáki, G., and Moser, E.I. (2013). Memory, navigation and theta rhythm in the hippocampal-entorhinal system. *Nat. Neurosci.* *16*, 130–138.
88. Reppas, J.B., Usrey, W.M., and Reid, R.C. (2002). Saccadic eye movements modulate visual responses in the lateral geniculate nucleus. *Neuron* *35*, 961–974.

89. Bosman, C.A., Womelsdorf, T., Desimone, R., and Fries, P. (2009). A microsaccadic rhythm modulates gamma-band synchronization and behavior. *J. Neurosci.* *29*, 9471–9480.
90. Loureiro, M., Cholvin, T., Lopez, J., Merienne, N., Latreche, A., Cosquer, B., Geiger, K., Kelche, C., Cassel, J.-C., and Pereira de Vasconcelos, A. (2012). The ventral midline thalamus (reuniens and rhomboid nuclei) contributes to the persistence of spatial memory in rats. *J. Neurosci.* *32*, 9947–9959.
91. Andrianova, L., Brady, E.S., Margetts-Smith, G., Kohli, S., McBain, C.J., and Craig, M.T. (2021). Hippocampal CA1 pyramidal cells do not receive monosynaptic input from thalamic nucleus reuniens. Preprint at bioRxiv. <https://doi.org/10.1101/2021.09.30.462517>.
92. Dolleman-van der Weel, M.J., Lopes da Silva, F.H., and Witter, M.P. (2017). Interaction of nucleus reuniens and entorhinal cortex projections in hippocampal field CA1 of the rat. *Brain Struct. Funct.* *222*, 2421–2438.
93. Krout, K.E., Loewy, A.D., Westby, G.W., and Redgrave, P. (2001). Superior colliculus projections to midline and intralaminar thalamic nuclei of the rat. *J. Comp. Neurol.* *437*, 198–216.
94. Scheel, N., Wulff, P., and de Mooij-van Malsen, J.G. (2020). Afferent connections of the thalamic nucleus reuniens in the mouse. *J. Comp. Neurol.* *528*, 1189–1202.
95. Morales, G.J., Ramcharan, E.J., Sundararaman, N., Morgera, S.D., and Vertes, R.P. (2007). Analysis of the actions of nucleus reuniens and the entorhinal cortex on EEG and evoked population behavior of the hippocampus. In 2007 29th Annual International Conference of the IEEE Engineering in Medicine and Biology Society (IEEE), pp. 2480–2484.
96. Eleore, L., López-Ramos, J.C., Guerra-Narbona, R., Delgado-García, J.M., Carlos Ló Pez-Ramos, J., Guerra-Narbona, R., and Delgado-García, J.M. (2011). Role of reuniens nucleus projections to the medial prefrontal cortex and to the hippocampal pyramidal CA1 area in associative learning. *PLoS One* *6*, e23538.
97. Jankowski, M.M., Passecker, J., Islam, M.N., Vann, S., Erichsen, J.T., Aggleton, J.P., and O'Mara, S.M. (2015). Evidence for spatially-responsive neurons in the rostral thalamus. *Front. Behav. Neurosci.* *9*, 256.
98. Wouterlood, F.G., Saldana, E., and Witter, M.P. (1990). Projection from the nucleus reuniens thalami to the hippocampal region: light and electron microscopic tracing study in the rat with the anterograde tracer *Phaseolus vulgaris*-leucoagglutinin. *J. Comp. Neurol.* *296*, 179–203.
99. Dolleman-Van Der Weel, M.J., Lopes Da Silva, F.H., and Witter, M.P. (1997). Nucleus reuniens thalami modulates activity in hippocampal field CA1 through excitatory and inhibitory mechanisms. *J. Neurosci.* *17*, 5640–5650.
100. Cobb, S.R., Buhl, E.H., Halasy, K., Paulsen, O., and Somogyi, P. (1995). Synchronization of neuronal activity in hippocampus by individual GABAergic interneurons. *Nature* *378*, 75–78.
101. Bush, D., Bisby, J.A., Bird, C.M., Gollwitzer, S., Rodionov, R., Diehl, B., McEvoy, A.W., Walker, M.C., and Burgess, N. (2017). Human hippocampal theta power indicates movement onset and distance travelled. *Proc. Natl. Acad. Sci. USA* *114*, 12297–12302.
102. Aghajian, Z.M., Schuette, P., Fields, T.A., Tran, M.E., Siddiqui, S.M., Hasulak, N.R., Tchong, T.K., Eliashiv, D., Mankin, E.A., et al. (2017). Theta oscillations in the human medial temporal lobe during real-world ambulatory movement. *Curr. Biol.* *27*, 3743–3751.e3.
103. Stewart, M., and Fox, S.E. (1991). Hippocampal theta activity in monkeys. *Brain Res.* *538*, 59–63.
104. Buzsáki, G. (2002). Theta oscillations in the hippocampus. *Neuron* *33*, 325–340.
105. Leszczynski, M., and Schroeder, C.E. (2019). The role of neuronal oscillations in visual active sensing. *Front. Integr. Neurosci.* *13*, 32.
106. Voloh, B., and Womelsdorf, T. (2016). A role of phase-resetting in coordinating large scale neural networks during attention and goal-directed behavior. *Front. Syst. Neurosci.* *10*, 18.
107. Cassel, J.C., Pereira de Vasconcelos, A., Loureiro, M., Cholvin, T., Dalrymple-Alford, J.C., and Vertes, R.P. (2013). The reuniens and rhomboid nuclei: neuroanatomy, electrophysiological characteristics and behavioral implications. *Prog. Neurobiol.* *111*, 34–52.
108. Dolleman-Van Der Weel, M.J., Griffin, A.L., Ito, H.T., Shapiro, M.L., Witter, M.P., Vertes, R.P., and Allen, T.A. (2019). The nucleus reuniens of the thalamus sits at the nexus of a hippocampus and medial prefrontal cortex circuit enabling memory and behavior. *Learn. Mem.* *26*, 191–205.
109. Xu, W., and Südhof, T.C. (2013). A neural circuit for memory specificity and generalization. *Science* *339*, 1290–1295.
110. McKenna, J.T., and Vertes, R.P. (2004). Afferent projections to nucleus reuniens of the thalamus. *J. Comp. Neurol.* *480*, 115–142.
111. Rutishauser, U., Schuman, E.M., and Mamelak, A.N. (2006). Online detection and sorting of extracellularly recorded action potentials in human medial temporal lobe recordings, in vivo. *J. Neurosci. Methods* *154*, 204–224.
112. Chandravadia, N., Liang, D., Schjetnan, A.G.P., Carlson, A., Faraut, M., Chung, J.M., Reed, C.M., Dichter, B., Maoz, U., Kalia, S.K., et al. (2020). A NWB-based dataset and processing pipeline of human single-neuron activity during a declarative memory task. *Sci. Data* *7*, 78.
113. Groppe, D.M., Bickel, S., Dykstra, A.R., Wang, X., Mégevand, P., Mercier, M.R., Lado, F.A., Mehta, A.D., and Honey, C.J. (2017). iELVis: an open source MATLAB toolbox for localizing and visualizing human intracranial electrode data. *J. Neurosci. Methods* *281*, 40–48.
114. Patel, K., Katz, C.N., Kalia, S.K., Popovic, M.R., and Valiante, T. (2020). Volitional control of individual neurons in the human brain. Preprint at bioRxiv.
115. Torres-Gomez, S., Blonde, J.D., Mendoza-Halliday, D., Kuebler, E., Everest, M., Wang, X.J., Inoue, W., Poulter, M.O., and Martinez-Trujillo, J. (2020). Changes in the proportion of inhibitory interneuron types from sensory to executive areas of the primate neocortex: implications for the origins of working memory representations. *Cereb. Cortex* *30*, 4544–4562.
116. Lemon, R.N., Baker, S.N., and Kraskov, A. (2021). Classification of cortical neurons by spike shape and the identification of pyramidal neurons. *Cereb. Cortex* *31*, 5131–5138.
117. Salvucci, D.D., and Goldberg, J.H. (2000). Identifying fixations and saccades in eye-tracking protocols. In Proceedings of the Symposium on Eye Tracking Research & Applications – ETRA '00, pp. 71–78.
118. Andersson, R., Larsson, L., Holmqvist, K., Stridh, M., and Nyström, M. (2017). One algorithm to rule them all? An evaluation and discussion of ten eye movement event-detection algorithms. *Behav. Res. Methods* *49*, 616–637.
119. Kovach, C.K., Tsuchiya, N., Kawasaki, H., Oya, H., Howard, M.A., and Adolphs, R. (2011). Manifestation of ocular-muscle EMG contamination in human intracranial recordings. *Neuroimage* *54*, 213–233.

## STAR★METHODS

### KEY RESOURCES TABLE

REAGENT or RESOURCE	SOURCE	IDENTIFIER
Software and algorithms		
MATLAB R2020	The MathWorks	RRID: SCR_001622; <a href="http://www.mathworks.com/products/matlab/">http://www.mathworks.com/products/matlab/</a>
Data Viewer	SR Research	RRID: SCR_009602; <a href="https://www.sr-research.com/">https://www.sr-research.com/</a>
Custom MATLAB scripts for analysis and statistical tests	This paper	Code is available via github: <a href="https://github.com/katzchai/CD_saccade_related_inhibition_MTL">https://github.com/katzchai/CD_saccade_related_inhibition_MTL</a> <a href="https://zenodo.org/badge/latestdoi/495560699">https://zenodo.org/badge/latestdoi/495560699</a>

### RESOURCE AVAILABILITY

#### Lead contact

Further information and requests should be directed to and will be fulfilled by the Lead Contact, Taufik Valiante ([taufik.valiante@uhn.ca](mailto:taufik.valiante@uhn.ca)).

#### Materials availability

This study did not generate new unique reagents

#### Data and code availability

All original code has been deposited at Zenodo and is publicly available as of the date of publication. DOIs are listed in the [key resources table](#).

All data reported in this paper that can be will be shared by the [lead contact](#) upon request and in accordance with the REB protocol.

### EXPERIMENTAL MODEL AND SUBJECT DETAILS

Eleven individuals with medically refractory epilepsy participated in this study (Table 1). As part of their clinical assessment, sEEG electrodes (Ad-Tech Medical, WI, USA) were implanted in clinically-determined sites to assess their candidacy for surgical resection of an epileptogenic focus. If patients provided written research consent to microwire recordings, then the sEEG macro-electrodes were supplemented with microwires (Ad-Tech Medical, WI, USA). Microwire implants and all recordings were approved by the Research Ethics Board of the University Health Network

### METHOD DETAILS

#### Experimental design

The terms "neuron" and "unit" are used interchangeably. To characterize neuronal activity in the time interval surrounding saccades, we developed a task that involved image presentation and target search (Figure 1A) to engage participants in generating saccades. The encoding session was divided into 40 trials, each consisting of a fixation cross (1 second), followed by presenting a scene image. Each scene contained four copies of one of two unrelated objects, i.e., targets, that were unrelated to the scene. Participants were instructed to view the individual, serially-presented scene and find as many targets within the scene as possible. If they found all four targets, participants were instructed to continue to move their eyes through the scene to remember and associate the target with the scene. Each scene image was presented for four seconds, after which participants were asked how many targets they found. The trials were grouped into blocks of five trials, with each block having the same embedded target. Following the encoding session, participants were presented with instructions on the ensuing retrieval session. The data presented here is based solely on eye movements during the encoding session.

Patients reclined upright in their clinical beds with a laptop computer placed at a comfortable viewing distance in front of them. An infrared, video-based eye-tracker (EyeLink Duo; SR Research, Osgoode, Canada) was used to monitor and record their eye movements throughout the task (see below for details on eye-tracking).

## Electrophysiology

### Acquisition and localization

Each commercially –available, Behnke–Fried Macro–Micro electrode (Ad-Tech Medical, Racine, MN) had 8 or 9 macro electrodes along the electrode shaft and a bundle of 8 embedded microwires plus one ground/reference microwire protruding from the tip.<sup>111</sup> Patients with MTL electrodes with or without electrodes in other anatomical locations specified by the pre-implantation hypothesis were included in this study. Data were recorded with a 128-channel Neuralynx Atlas Data Acquisition System (Neuralynx, Bozeman, MT). The microelectrodes were sampled at 32kHz, with a 16-bit resolution and were bandpass filtered in hardware between 0.1 and 8kHz. Each microwire signal was re-referenced locally to one of the eight wires on the same bundle as we have done previously.<sup>112</sup> Electrode localization was performed by co-registering pre-op MRI with post-op CT using the IELVIS toolbox.<sup>113</sup> Electrodes were localized and visualized in the MTL structures across patients (Figure 1C; For occipital localizations, see Figure S2A).

### Spike detection and sorting

For offline spike detection, all microelectrode channels were bandpass filtered between 300–3000Hz. Spikes were subsequently detected using local energy measurement threshold crossings, calculated by convolving the raw signal with a kernel with an approximate width of an action potential.<sup>114</sup> All detected spikes were sorted using the open-source, semiautomatic template-matching algorithm OSort, which has been used extensively in the literature.<sup>111</sup> Briefly, spikes are detected using threshold crossings of a bandpassed filtered signal. For each spike, 2.5ms is extracted and upsampled with interpolation. A residual sum of squares is calculated to measure distance between neurons and cluster them for separation of units. Similar to our previous work,<sup>51,53</sup> we classified clusters as putative single neurons using the following criteria: (1) minimal/no violation of refractory period; (2) shape of the inter-spike interval distribution (units with more than 3% of their ISI distribution below 3ms were rejected); (3) shape of the waveform; (4) separation from other clusters; and, (5) stability of firing rate (assessed by comparing the average firing rate of the neuron to multiple null distributions obtained by randomly sampling 400ms and 5s epochs from each neuron's spike train). Groups that appeared similar to one another were merged. For extra quality control, neurons with firing rates lower than 0.07Hz were subsequently removed. Clusters that were either contaminated with noise or failed to meet the criterion described above were rejected. For the accepted clusters, the individual waveforms, along with the timestamp of each spike and its cluster definition, were saved. The insert of Figure 1C shows the total cells from each location detected in MTL (neuronal activity from occipital locations is shown in Figure S2A).

### Waveform analysis

The shape of a waveform suggests which type of neuron produced it. Narrow spiking is typically attributed to inhibitory parvalbumin expressing neurons, and while there are broad spiking inhibitory neurons that express other markers, pyramidal neurons make up the large proportion of all broad spiking neurons.<sup>75</sup> For each neuron, we calculated the spike width by measuring the trough-to-peak timed as the duration between the first negative peak of the mean waveform ('trough') and the first positive peak after the trough.<sup>49</sup> The mean waveform is obtained by averaging all the waveforms assigned to a particular cluster. We classified the neurons as broad and narrow spiking using an approach previously described by Gomez-Torres et al. 2020.<sup>115</sup> In this approach, we fit our distribution of spike-widths with a Gaussian Mixture model with a number of gaussians that minimized the Akaike Information Criterion (5 Gaussians in this case Figure S5). We chose the cut-off as the inflection point between the first gaussian and the remainder of the distribution. This resulted in a cut-off value of 0.453ms. We classified all neurons with a peak to trough width lower than 0.453ms as narrow and the rest as broad spiking. It should be noted that the broad spiking neurons had a multimodal spike-width distribution, likely due to a heterogeneity of neurons that contributed to this category. For instance, in addition to pyramidal neurons, previous studies have found that parvalbumin negative interneurons can also have broad spikes.<sup>116</sup> For the purpose of our investigation, we did not further classify the sub-groups within the broad spiking category.

### Analysis of eye-tracking data

The SR Research eye-tracking system was used to track participants' eye movements. The eye-tracker was placed at the bottom of the screen and connected via ethernet to a separate laptop running the behavioural task using Presentation software (NeuroBehavioral Systems, Albany, CA, USA). All participants first underwent a 13-point calibration and 9-point validation test (EyeLink Portable Duo sampled at 1000Hz, from SR Research).

Eye movements were detected using SR Research's built-in software that uses an Identification by Velocity-Threshold (IVT) algorithm. This algorithm is a velocity-based method that separates fixations and saccades based on the distance between the current and next points.<sup>117</sup> To be considered a saccade, the velocity between points must exceed 30 deg/sec. When ten eye-tracking algorithms' accuracy at detecting saccades on a sample-by-sample basis (as we do here) were compared, the IVT algorithm was second closest to human detection for saccade events.<sup>118</sup> An example of saccades and an image is presented in Figure 1A.

The saccade's horizontal direction was determined by subtracting its ending point from the starting point. We coded the top left of an image as the origin, so if the saccade's ending point was less than the starting point (a negative value), it was considered leftward. In contrast, if it was positive, it was considered rightward (Figure 1B).

## QUANTIFICATION AND STATISTICAL ANALYSIS

All analyses were performed offline using custom scripts in MATLAB.

Nonparametric bootstrapping was performed for neural modulation. Statistical tests on neural latencies were either parametric (paired t test, one sample t tests) or non-parametric (Wilcoxon Signed-Rank Test or Wilcoxon Rank-Sum Test), based on the results



of the Lilliefors normality test. A binomial test was used to determine the significance of modulation of neurons and directional neurons from the overall number of neurons. A Fisher's exact test was used to compare the distribution of modulated neurons to determine significance.

### Analysis of electrophysiological data

#### Analyzing saccade onset responses

Spike timestamps from offline sorted neurons were used to create binary spike trains. We then extracted 2-second epochs centred on each saccade onset for each of the sorted neurons. The spike counts were binned into 50ms bins to extract the instantaneous firing rate. The average firing rate in the perisaccadic intervals (i.e. average across all saccades and surrounding 400ms around saccade onset consisting of 8 bins of 50ms each) were used to assess modulation (Figure 2A).

To determine the statistical significance of the average peri-saccadic firing rates, we used a non-parametric permutation method. More specifically, for each session, we extracted the same number of 400ms epochs (four example intervals in dark blue shown in Figure 2A) as the number of saccades in the session, only at random time points. By averaging across these epochs, and then averaging across time within the 400ms average epoch (i.e. across the 8 bins of 50ms each), we calculated a single shuffled peri-saccadic firing rate. We repeated this process 1000 times to create a shuffled null distribution of mean peri-saccadic firing rates. If the actual mean perisaccadic firing rate for a given neuron exceeded the 97.5<sup>th</sup> percentile of the shuffled null distributions, it was considered a significant perisaccadic increase. Similarly, if the actual mean perisaccadic firing rate for a given neuron was lower than the 2.5<sup>th</sup> percentile of the control null distribution, it was considered a significant perisaccadic decrease (Figure 2A, inset).

As a result, neurons were classified into one of three groups – (1) non-modulated (no significant increase or decrease in firing rate during the perisaccadic interval), (2) perisaccadic increase (significant increase in firing rate during the perisaccadic interval), and (3) perisaccadic decrease (significant decrease in firing rate during the perisaccadic interval (Figure 2B)). The population activity was calculated by averaging all modulated neurons' average firing rate aligned to saccade onset, separately for each category (decrease or increase). The percent change was calculated based on the ratio of the average firing rate per neuron during the saccade period, divided by the mean firing rate in the randomized control periods (Figure S1C). Then that percent change was averaged across all neurons. We also calculated the perisaccadic firing probability density by fitting all spike timestamps in 2 seconds around each saccade with a kernel distribution with a bandwidth of 50ms. This probability density was then upsampled (using a bicubic spline interpolation) to obtain a 1ms resolution. The maxima and minima of this upsampled firing probability density were used to calculate the peak and trough latency of the firing rate increases and decreases, respectively, for the saccade-modulated units (Figure S1C, insert). A histogram of the latencies is also presented in Figure S3C and Table S1.

Although the interest in the present study focused on single unit saccadic modulation of MTL structures, in two participants, we had the unique opportunity to record activity from the occipital cortices (OCC) simultaneously. Therefore, we performed a unit-by-unit analysis from neurons acquired in this area, shown in the supplementary material, in a manner identical to that previously described for MTL neurons. However, we added a fourth classification for OCC neurons: rebound modulation. Neurons classified as having rebound modulation demonstrated a significant decrease in firing rate followed by a significant increase in firing rate. To evaluate significant decreases and increases within the 400ms perisaccadic window, we created a shuffled null distribution of maxima and minima values. This was done by extracting 400ms epochs at random times, matching the number of saccades in each session. We averaged these epochs to obtain a mean 400ms epoch. The maximum value across the 400ms (i.e. one of the eight 50ms bins) in this mean epoch was added to the maxima null distribution, and the minimum value across the 400ms was added to the minima null distribution. This process was repeated 1000 times to generate a complete maxima and minima null distribution. We identified if any of the eight 50ms bins in the actual mean peri-saccadic firing rate exceeded the 97.5<sup>th</sup> percentile of the maxima null distribution and if any of the 50ms bins fell below the 2.5<sup>th</sup> percentile of the minima null distribution. Neurons that demonstrated significant decreases followed by significant increases were marked as rebound neurons. Note that the classification as a rebound neuron superseded the other classifications. It should also be noted that in the rebound classification, multiple comparisons were not necessary since we compared the eight 50ms bins with a distribution of maxima and minima across the 400ms windows. This comparison is conservative since each of the eight bins is compared to the null distribution corresponding to its position in the 400ms window and the maximum and minimum values across the entire 400ms window in the shuffled null distribution. Note that none of the MTL units demonstrated a characteristic rebound firing.

To determine if the amplitude of the post-saccade event-related potentials (ERPs)<sup>15</sup> was related to firing rate changes, post-saccade ERPs were computed from voltage traces of the most distal macroelectrode (i.e., the one closest to the corresponding microelectrodes). Each macroelectrode had a 200Hz lowpass filter and was downsampled to 1000Hz. A 60 Hz notch filter was applied to reduce environmental noise from the signal. Each macroelectrode ERP was normalized by dividing by the standard deviation of the voltage trace of that electrode during the entire recording. The ERPs found to have a reversed polarity were flipped to obtain a positive waveform (MTL= 1/58; OCC= 5/8). We eliminated responses from electrodes with large artifacts in the ERP and, therefore, considered open or broken channels (MTL= 4/58; OCC= 0). The subsequent average from all electrodes was calculated and plotted for MTL (Figure S1D) and occipital electrodes (Figure S2G). The root mean squared (RMS) amplitude of the normalized ERP was then calculated from 10ms-510ms post saccade onset. This time was chosen as it is in line with the significant portions of the saccade ERP from our earlier work.<sup>15</sup>

Previous iEEG work has identified differences in responses based on the direction of saccade relative to recording location,<sup>41</sup> even as it relates to potential oculomotor artifact.<sup>119</sup> Therefore, we further labelled saccades as ipsiversive if the saccade's direction was

towards the side of the recording electrode's hemisphere or contraversive if the saccade's direction towards the opposite hemisphere. We repeated the categorization and ERP analyses described above, now separating events based on the saccade direction. Additionally, a paired t test was used to compare ipsiversive to contraversive saccade RMS distributions. Finally, separating ipsiversive and contraversive saccades, we calculated the Spearman rank correlation between the ERP RMS amplitude and the percent change in firing (decreases only) of the corresponding modulated neurons close to those electrodes. Single unit modulation was similar across the MTL structures, so they were grouped together for further analysis (Figure S3).

#### **Analyzing Image Onset Responses**

Single unit responses to image onset were analyzed in a window between 200 and 1700ms after image onset, in line with previous single-unit literature.<sup>49</sup> Neurons were marked as modulated by image onset if their mean firing rate in this window significantly increased or decreased compared to the corresponding null distribution (Figure 2C). Control null distributions for image onset analysis consisted of 1500ms periods of spike trains at randomized timepoints. The population activity was also calculated for neurons that increased or decreased their firing rate to image onset (Figure S1G).